



<b>Publication Year</b>	2016
<b>Acceptance in OA</b>	2020-05-04T10:42:49Z
<b>Title</b>	Realization and drive tests of active thin glass x-ray mirrors
<b>Authors</b>	SPIGA, Daniele, Barbera, Marco, COLLURA, Alfonso, BASSO, Stefano, CANDIA, Roberto, CIVITANI, Marta Maria, DI CICCA, Gaspare, LO CICERO, UGO, Lullo, Giuseppe, Pellicciari, Carlo, SALMASO, Bianca, SCIORTINO, LUISA, VARISCO, Salvatore
<b>Publisher's version (DOI)</b>	10.1117/12.2231284
<b>Handle</b>	<a href="http://hdl.handle.net/20.500.12386/24422">http://hdl.handle.net/20.500.12386/24422</a>
<b>Serie</b>	PROCEEDINGS OF SPIE
<b>Volume</b>	9965

# Realization and drive tests of active thin glass X-ray mirrors

D. Spiga<sup>1§</sup>, M. Barbera<sup>2,3</sup>, A. Collura<sup>3</sup>, S. Basso<sup>1</sup>,  
R. Candia<sup>3</sup>, M. Civitani<sup>1</sup>, G. Di Cicca<sup>3</sup>, U. Lo Cicero<sup>3</sup>,  
G. Lullo<sup>2</sup>, C. Pelliciarì<sup>1</sup>, B. Salmaso<sup>1</sup>, L. Sciortino<sup>2</sup>, S. Varisco<sup>3</sup>

<sup>1</sup>INAF – Osservatorio Astronomico di Brera, Via Bianchi 46, 23807 Merate (Italy)

<sup>2</sup>Università degli Studi di Palermo, Via Archirafi 36, 90123 Palermo (Italy)

<sup>3</sup>INAF - Osservatorio Astronomico di Palermo, Piazza del Parlamento 1, 90134 Palermo (Italy)

## ABSTRACT

A technique to obtain lightweight and high-resolution focusing mirror segments for large aperture X-ray telescopes is the hot slumping of thin glass foils. In this approach, already successfully experimented to manufacture the optics of the NuSTAR X-ray telescope, thin glasses are formed at high temperature onto a precisely figured mould. The formed glass foils are subsequently stacked onto a stiff backplane with a common axis and focus to form an XOU (X-ray Optical Unit), to be later integrated in the telescope optic structure. In this process, the low thickness of the glass foils guarantees a low specific mass and a very low obstruction of the effective area. However, thin glasses are subject to deformations that may arise at any stage of the production process, thereby degrading the angular resolution. To solve this problem, several groups are working on the possibility to correct the mirror profile post-manufacturing, using piezoelectric elements exerting a tangential strain on the non-optical side of the glass mirrors. In this paper we show the results of the approach we have adopted, based on the application of piezoceramic patches on the backside of thin glass foils, previously formed by hot slumping. The voltage signals are supplied to the piezoelectric elements by a system of electrodes deposited on the same side of the mirror via a photolithographic process. Finally, the matrix of voltages to be used to correct the mirror shape can be determined in X-rays illumination by detection of the intra-focal image and consequent reconstruction of the longitudinal profile. We describe the production of some active mirrors with different arrangements of piezoelectric elements and the X-ray tests performed at the XACT X-ray facility to determine the optimal actuator geometry.

**Keywords:** X-ray mirrors, active optics, thin glass mirrors, piezoelectric actuators

## 1. INTRODUCTION

Manufacturing large, lightweight, and high angular resolution optical modules will represent the challenge of the next years for astronomical X-ray optics: the current requirements for e.g., the ATHENA X-ray telescope,<sup>[1]</sup> currently selected by ESA for the L2 launch slot, are a 2 m<sup>2</sup> effective area at 1 keV with an angular resolution of 5 arcsec HEW (Half Energy Width), obtained by populating a 3 m wide module with co-focal modular elements (XOU, X-ray Optical Units) with high angular resolution. The large dimensions of the optics and the dense mirror nesting needed to meet the effective area requirements require us to adopt lightweight materials, such as glass or silicon; for ATHENA, the baseline technology adopted is Silicon Pore Optics<sup>[2]</sup> (SPO), developed by ESA/ESTEC and Cosine since 2004, and still ongoing. However, Slumped Glass Optics (SGO) represent a viable alternative to manufacture high-resolution, lightweight and densely nested optical modules. An advantage of SGO is, for example, the larger size of formed foils and the lower obstruction caused by the spacers (“ribs”) used to keep the reflective surfaces at the correct distance. In this approach, already experienced for the NuSTAR telescope,<sup>[3]</sup> thin foils of glass are formed at high temperature onto a precisely figured mould and stacked to form an XOU.<sup>[4]</sup> The ribs also provide the mechanical stiffness to the XOU needed to maintain its shape during the operation. For the ATHENA (formerly IXO) X-ray telescope, the SGO technology has been developed at INAF/OAB under ESA/ESTEC contract in 2009-2013, and in parallel at MPE (Garching, Germany), following two different methodologies (*direct* slumping at OAB<sup>[10]</sup> and *indirect* slumping at MPE<sup>[10]</sup>). In both cases, as well as for SPOs, it was proven that an optical design based on SGO is suitable to provide the requested effective area/mass ratio.

---

§ contact author: [daniele.spiga@brera.inaf.it](mailto:daniele.spiga@brera.inaf.it), phone +39-02-72320427

In the direct slumping methodology, the longitudinal profile of the X-ray mirror is subject to non-negligible errors that have been continuously reduced by a proper optimization of the slumping setup (mould height, intensity and duration of the pressure exerted, surface cleanliness, settings of the slumping cycle...). For example, even if the surface smoothness of the reflective surface can be damaged by the contact of the mould, the surface degradation could be reduced<sup>[7]</sup> to levels causing negligible scattering below 1 keV. Regarding figure defects, they are partly corrected by the development of an integration process,<sup>[3]</sup> which endows the slumped foils with the Wolter-I profile of accurately figured integration moulds. Fixing the stack on the glass via stiffening glass ribs, the nominal shape is imparted to the optical surface at the rib locations. Because of the glass elastic properties, however, the correction is only partial, especially for defects ranging on a few centimeters of lateral scale in the longitudinal direction. The residual profile error is also a function of the distance from the nearest rib: more exactly, it is maximum amid adjacent ribs, whereas only at the rib location the profile copies almost exactly the nominal shape imparted by the integration mould.<sup>[8]</sup> As a result, the expected angular resolutions of slumped glass mirrors are approaching the target of 5 arcsec HEW, but are still far from the sub-arcsec resolutions envisaged for some mission concepts as the X-ray Surveyor project.<sup>[9]</sup>

Even if further process improvements are surely possible, several groups worldwide are at work on the possibility to actively correct the mirror profile after forming. However, the dense nesting, typical of X-ray optics, does not permit using normal actuators, as commonly done in optical astronomy. In contrast, using piezoelectric elements acting *tangentially*, i.e., exerting a strain in a direction parallel to the surface on the rear of the glass foil, the local curvature of the mirror can be changed and profile errors corrected. For example, the group at CfA/SAO is working on the deposition of the piezoelectric layer by sputtering<sup>[10]</sup> on the backside of the mirrors and some prototypes, also using slumped glass foils at INAF/OAB,<sup>[7]</sup> have been produced and successfully tested.

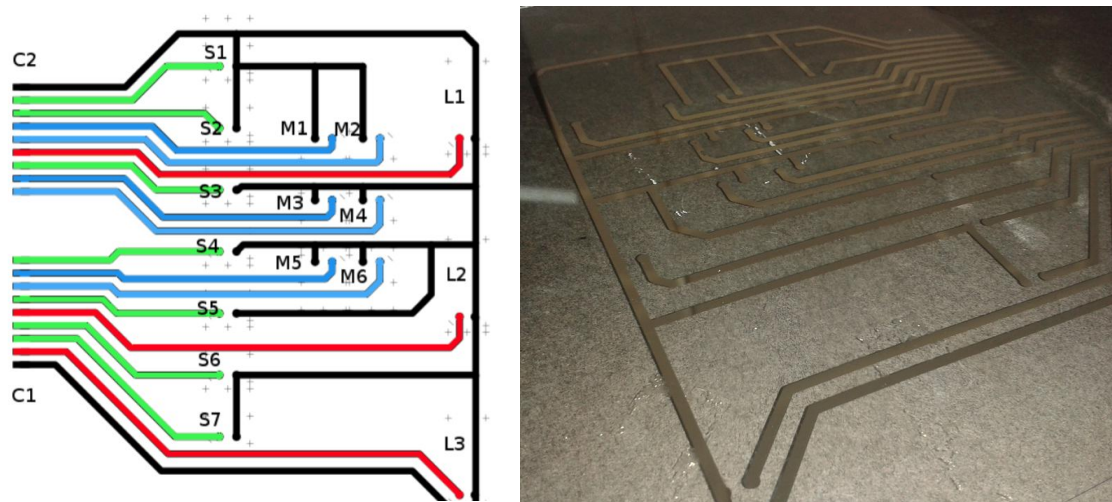


Fig. 1: (left) design of the printed circuit to drive the piezo array in the first prototype. The green contacts feed small (16 × 13 mm) piezoelectric patches in line along an anti-rib, denoted as S1 to S7; the blue electrodes provide voltages to M1 to M6 piezo elements of the same size, but arranged in a 2×3 matrix; the red contacts power the long actuators (L1, L2, and L3, 50 mm × 11 mm). The C1 and C2 electrodes are grounded contacts. (right) the E43 glass with the printed electrodes.

In the approach envisaged in the context of the *AXYOM (Adjustable X-ray optics for astrOnomy)* project,<sup>[11]</sup> we have adopted commercial piezoelectric elements to be glued on the non-reflective layer of slumped glass foils. The slumping process of EAGLE-XG (Corning) thin glasses is described in another paper of this volume,<sup>[7]</sup> and the piezoelectric elements that have been selected are flexible piezoceramic transducers<sup>[12]</sup> available from *Physik Instrumente*. A first experiment<sup>[13]</sup> was performed on a simple prototype<sup>[14]</sup> with two piezoceramic patches mod. P-876.SP1, with a 16 mm × 13 mm size and a thickness of only 200 μm to avoid X-ray obstruction in a mirror stack. These piezoelectric elements are qualified for vacuum applications and can operate in a voltage range from -100 V to +400 V, much larger than the values expected for a correction of mirror defects up to a maximum amplitude of a few microns.

In this paper we report the development of the project, in which we have produced two additional active mirrors, with a higher number of piezo elements. Since profile metrology is hard to perform in densely nested mirror stacks, we performed X-ray tests in intrafocal setup at the 35 m long X-ray facility XACT<sup>[15][16]</sup> at INAF/OAPA. The mirror image, when observed intra-focus, resembles an arc with intensity modulations in the radial direction, mostly determined by the

longitudinal figure errors. By means of an iterative process,<sup>[8]</sup> it is possible to retrieve the actual mirror profile and so compute the voltages to be provided to the piezos, provided that the intensity striations remain quasi-parallel and do not cross each other. We therefore show the results of the X-ray tests in XACT, and how the deformations induced by the glue can be partially corrected energizing the piezoelectric patches.

## 2. ACTIVE X-RAY MIRROR PAIR (XMP)

### 2.1. XMP realization

We have realized an X-ray mirror pair in Wolter-I configuration, using the setup already available at INAF/OAB to form cylindrical mirror segments with 0.4 mm thickness, 1 m radius, and 200 mm × 200 mm lateral dimensions.<sup>[7]</sup> The parabolic and hyperbolic integration moulds installed in the Integration Machine (IMA) allow us endowing the cylindrical foils with a parabola/hyperbola profile with a 20 m combined focal length.<sup>[4]</sup> The glass foils are integrated onto a double conical backplane via glass ribs: for the prototypes integrated in this project, the backplane is in aluminum, which has a thermal expansion coefficient (CTE) different from the one of the glass: therefore, to avoid deformations caused by the CTE mismatch, the mirror module shall be tested at the same temperature at which it was integrated.

With respect to the mirror described in the previous paper,<sup>[14]</sup> the circuit was completely re-designed: the scope of this test was to determine which piezo format and arrangement is the most effective in terms of surface deformation and profile actuation. We have therefore actuated the three central sectors between the ribs, the ones less affected by the connector loads applied on the glass sides, with different piezo geometries:

- 1) a linear array of 7, equally-spaced small (16 mm × 13 mm, from now on “S”- type piezos) piezoelectric patches, on the median line between the ribs;
- 2) a 2 × 3 array (“M”- type piezos) of patches with the same size;
- 3) a linear array of 3 longer (from now on “L”- type piezos, mod. K015 (50 mm × 11 mm).

The distribution of electrodes required to feed the piezo system is sketched in Fig. 1, left. The circuits were deposited on the backside of two slumped glass foils (named E41 and E43) with surface roughness fulfilling the prescribed tolerances,<sup>[7]</sup> using the photolithographic process developed at INAF/OAPA - UniPA and described in detail in a previous work.<sup>[14]</sup> One of the mirror plates with the deposited contacts is shown in Fig. 1, right. The electric tracks have been reduced in thickness, aiming to avoid mirror deformations caused by the stress in the metallic layer: in fact, measurements done with the CUP profilometer at OAB (Fig. 2) showed that the metallic tracks have left no remarkable imprint on the optical surface. For the subsequent mirror plates, in addition, the procedure was modified to ensure a better uniformity of the photoresist<sup>[17]</sup> and so reduce the risk of interrupted contacts.

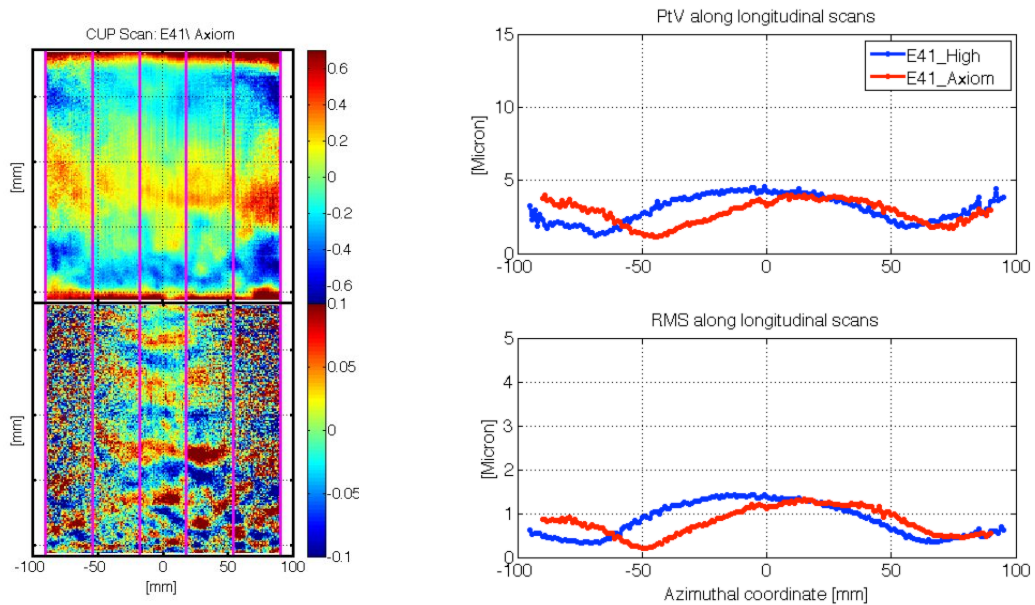


Fig. 2: (left) CUP map of the E41 coated glass after depositing the electrical contacts, without and with 8<sup>th</sup> order polynomial detrend. (right) the PV and of the rms value of each longitudinal scan. No imprint of the electrode pattern is visible.

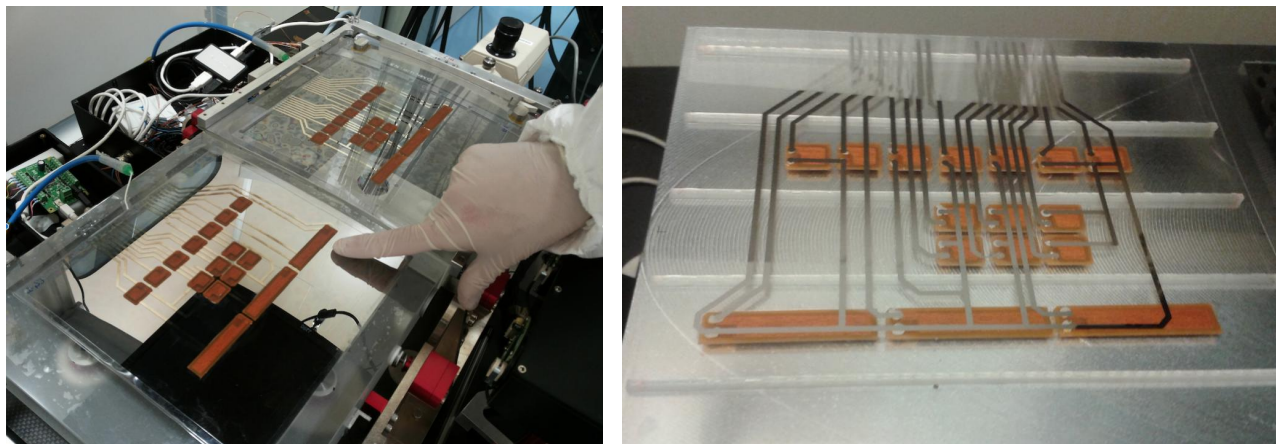


Fig. 3: (left) the E41 and E43 glass foils being integrated on the IMA, after gluing the piezoelectric patches in electrical contact with the metallic tracks. (right) closer view on the E43 glass after integration, showing the electrode paths and the ribs glued on the foil and the backplane.



Fig. 4: the complete XMP. The two segments are in Wolter-I configuration but have been tested separately under X-rays. The parabola (on the right) was coated with a thin layer of titanium to enable profile measurements with the LTP and so understand if the deformations induced by the active elements are sufficient to perform the local shape correction. The hyperbola (on the left) has been left uncoated to avoid some possible deformation caused by the stressed coating.

The patterned slumped glasses have been forced in contact with the integration moulds in the IMA and the piezoelectric elements have been glued in their position (Fig. 3) using the low-shrinkage (0.03%) and vacuum-qualified epoxy glue Masterbond EP30-2, routinely used to integrate our glass plates: the glue layer thickness can be estimated of about 50  $\mu\text{m}$ . The electrical contact between the electrodes and the soldered pads of the piezos was ensured by two droplets of conductive glue. The ribs were finally fixed to the backplane and the module completed fixing the ribs to the glass. After curing the glue during 48 h, the XMP was separated from the moulds (Fig. 4) and ready for test.

Finally, a dedicated electronic was developed to feed the piezos individually in the  $-90\text{ V}$  to  $+90\text{ V}$  range. A description of the driving electronics is detailed in another paper of this volume.<sup>[17]</sup>

## 2.2. XMP profile measurements

Even if the feedback to the voltage array should be achieved directly in X-rays, the functionality of the piezos was tested before transporting the XMP to XACT. To this aim, some profile measurements with the LTP were taken on the parabolic segment activating a single piezo at a time, using a DC power supply ( $< 25\text{ V}$ ). The effect of the “S” array activation could be seen locally in the piezo area (Fig. 5, Fig. 6, Fig. 7). The measured profiles have been used to compute the expected intensity profile at 4700 mm distance, in order to estimate the visibility of profile changes in the intrafocal trace. Clearly, this kind of measurement was possible only because the mirrors were *not* stacked and because the parabolic segment was coated with a reflective layer of titanium. No LTP measurement would be possible on the uncoated mirror, because the reflection on the non-optical side would create a double reflected beam, disturbing the signal acquisition.

The results can be summarized as follows:

- In the “S” array, the effects are clearly seen *locally* in the profile, without noticeable global effects.
- The 7  $\mu\text{m}$  peak-to-valley value observed in the unactuated profile is much larger than usually measured in non-actuated mirrors. The shrinkage of the glue layer (50-70  $\mu\text{m}$  thick) is probably responsible for this deformation.
- The *simulated* intra-focal trace also shows a local displacement of the intensity peaks, from which the mirror reconstruction should be made possible.
- For the “L” and the “M” array, the deformation is much larger because the glue is much more concentrated (25  $\mu\text{m}$  for M, 35  $\mu\text{m}$  for the L), and the effects are no longer localized but tend to spread outside their area.

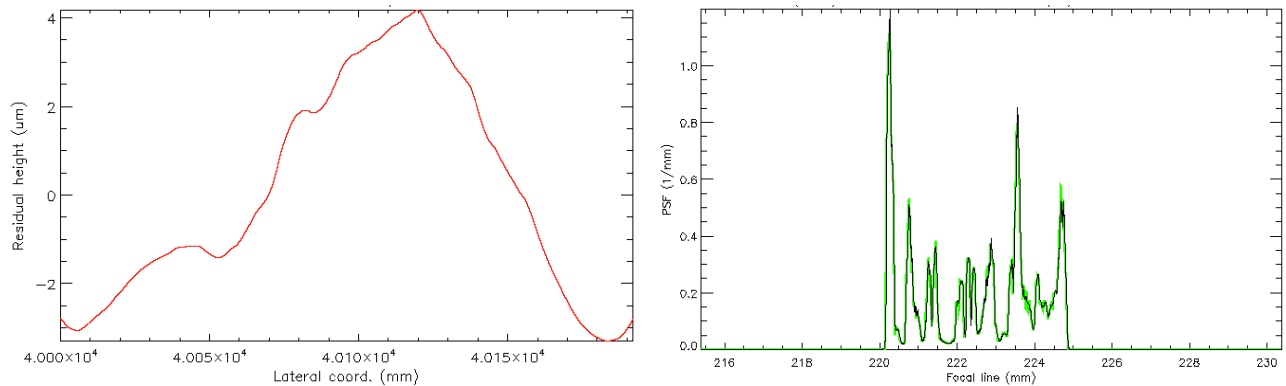


Fig. 5: (left) profile measurements with the LTP along the line passing by the S piezo array, without voltages applied. (right) intensity modulation in the intra-focal X-ray image at 4700 mm distance from the module, as expected from the LTP measurement.

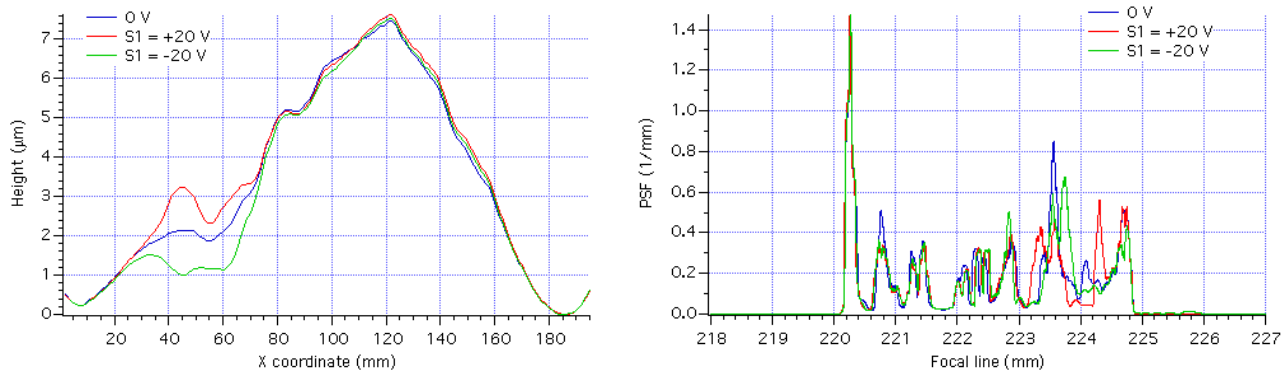


Fig. 6: (left) profile measurements with the LTP along the line passing by the S piezo array, with the piezo S1 activated at  $\pm 20$  V. (right) expected X-ray intensity peak displacement in the intra-focal image.

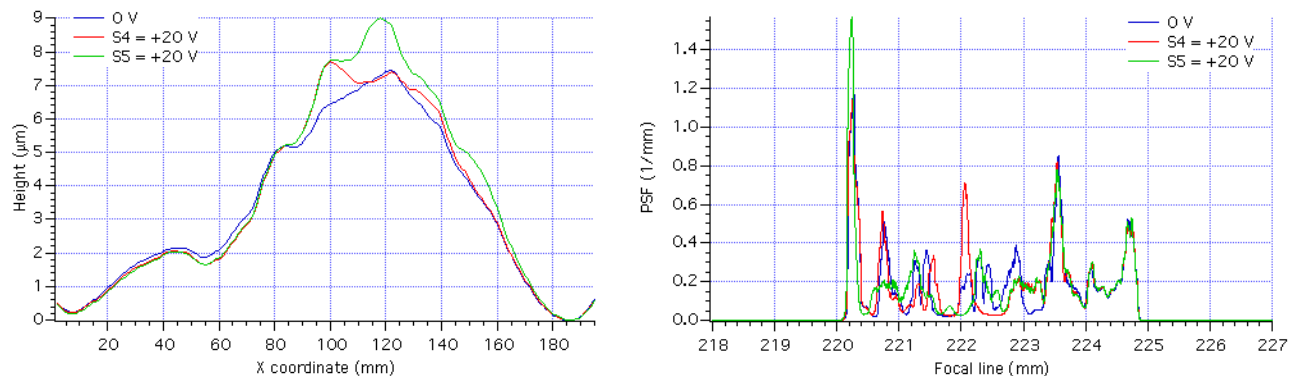


Fig. 7: (left) profile measurements with the LTP along the line passing by the S piezo array, with the piezos S4 and S5 activated at +20 V. (right) expected X-ray intensity peak displacement in the intra-focal image.

A 25  $\mu\text{m}$  P-V is hard to correct also using the maximum possible voltage (100 V), and the intra-focal measurements taken at XACT confirm this (Sect. 5.1). The glue shrinkage between the piezo and the glass therefore appears to be the main problem: in the second prototype manufactured, we have taken some actions to reduce this effect, and we have selected the “S” array configuration as the most interesting.

### 3. ACTIVE X-RAY SINGLE MIRROR (XSM)

The large deformation observed in the “L” and “M” array indicates that probably only a S-type array can be used to mitigate the deformation induced by the glue. To ascertain this, a FEM simulation was performed. The result is shown in Fig. 8, left: the central region, occupied by the rectangular array, is the most deformed one and probably the hardest to correct. Also the L piezos exhibit a relevant deformation, whereas the S region has the lowest distortion of the optical surface. Also the thickness of the glue, however, has a major impact: Fig. 8, right, shows that halving its thickness and avoiding spreading glue on non-activated locations contribute both to mitigate the shrinkage effect.

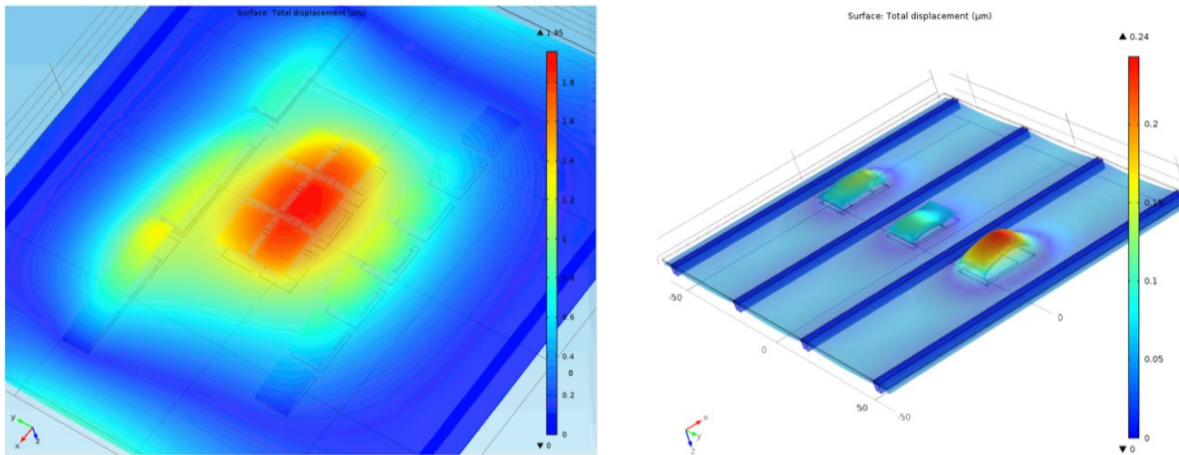


Fig. 8: finite element analysis, obtained via the COMSOL simulation program, of the XMP with a 50  $\mu\text{m}$  thickness of glue between the glass and the piezos. (left) The largest deformation, caused by the glue shrinkage, is located in correspondence to the “M” piezos. (right) different deformations induced by different glue thickness values. The central piezo was glued only in the active zone, avoiding the Kapton frame.

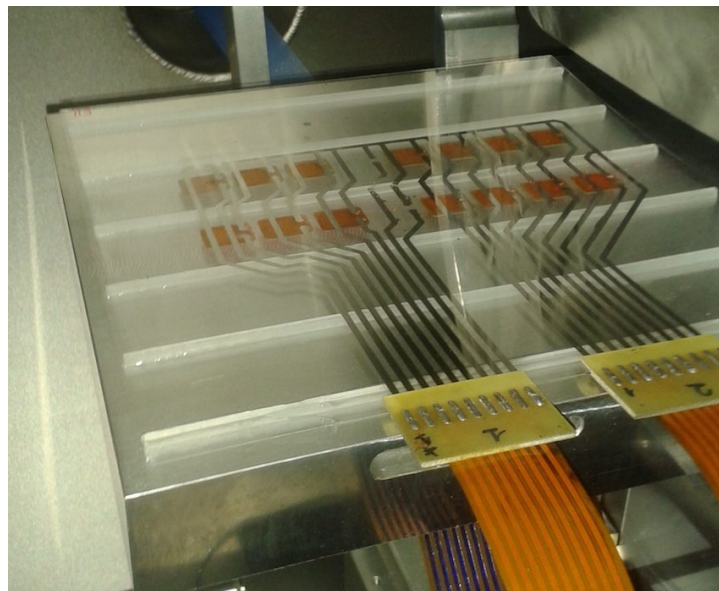


Fig. 9: the complete XSM. The slumped glass was activated with two lines of “S” piezos in two central sectors. Two flexible connectors have been specifically fabricated<sup>[17]</sup> to bring the required voltages to the piezoelectric elements in vacuum, via the deposited electrodes.

The XSM was therefore fabricated following these guidelines. It consists this time of a single, uncoated mirror plate with two arrays of 7 small piezos, along the central line of the two central sectors between consecutive ribs (Fig. 9). The integration procedure has been performed on the IMA as in the XMP case (Sect. 2.1) using the paraboloidal integration mould, excepting:

- 1) the reduced volume of the glue (approximately halved);
- 2) all the piezos glued together, keeping them aligned on an array of vacuum chucks fixed to a plexiglas slab;
- 3) higher pressure on the piezos exerted while the glue curing in order to reduce the thickness of the glue layer, using the weight of the plexiglas slab. In this way, the glued area is now limited to the sole active region;
- 4) the glue cured 5 days before releasing the vacuum to ensure a firmer grip and avoid possible deformations.

After vacuum release, the XSM was separated from the mould. No measurement with the LTP was possible because the mirror is uncoated, but we expected to see the mirror deformations directly in X-rays.

#### 4. EXPERIMENTAL SETUP AT THE XACT FACILITY

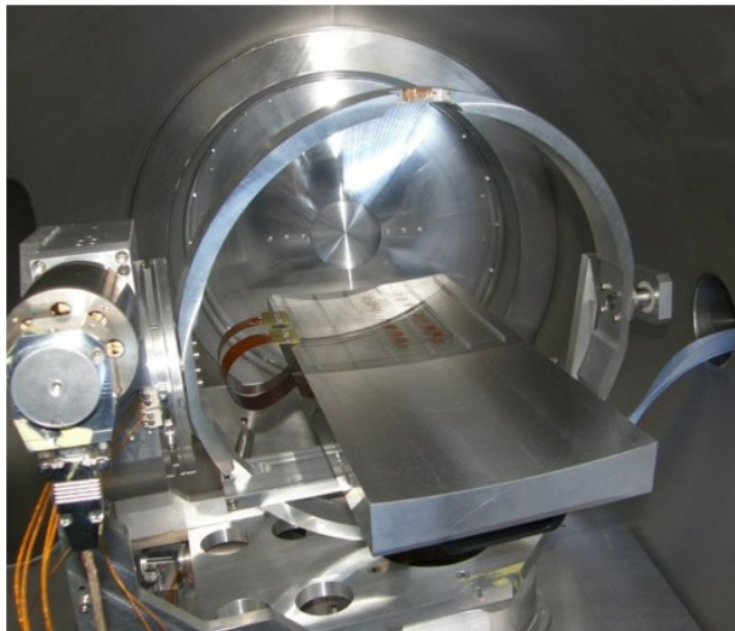


Fig. 10: the XSM mounted in the alt-az alignment stage in XACT. In this case, to minimize the distance between the optic and the microchannel plate (MCP) imaging detector, the alignment stage was mounted directly in the tube connecting the experimental chamber to the MCP.

The XACT X-ray facility in INAF/OAPA is widely described in previous papers.<sup>[15][16]</sup> we just remind here that even if the source is diverging (with a 35 m total range in high vacuum) and therefore a 20 m focal length cannot be accommodated (the source-to-detector distance should be at least 80 m to form an image), for the present need the divergence is almost irrelevant because the image is recorded in intra-focal location. In the testing campaign exposed here, we have mounted the XMP and the XSM in the XACT vacuum tube. To align the module in the 0.3 keV beam (the carbon  $K\alpha$  line), we have used the alt-az stage shown in Fig. 10, properly modified in order to support our modules; two axes are available to precisely adjust the rotation and the tilt of the optic with respect to the beam. The image is recorded in intra-focal position by a microchannel plate (MCP) detector with 4 cm field diam. and a spatial resolution of 0.1 mm. In order to minimize the intra-focal trace distortion, however, the optic had to be mounted very close to the MCP: the XMP was mounted in the closest possible position to the MCP (4700 mm), but still inside the standard experimental tank of XACT. In contrast, the XSM was mounted much closer (1100 mm), directly in the tube connecting the MCP to the rest of the facility.

The theoretical width of the intra-focal image depends on the incidence angle set on the mirror. This can be quite freely chosen within the total reflection range, because the profile reconstruction has to be done in single reflection, but the angle should always be known precisely. The XMP, being a double reflection module, could be aligned using the method described in a previous work,<sup>[8]</sup> i.e., firstly achieving the best alignment for double reflection and then increasing/reducing the incidence angle to isolate the parabola/hyperbola single reflection. In this case, the nominal

incidence angle for double reflection is 0.7 deg; hence, the module needed to be rotated by that angle to see the singly-reflected beams, at a 1.4 deg incidence angle. With this setting, the nominal intrafocal trace width is 5 mm. For the XSM, no doubly reflected beam could be adopted as reference position, and the real incidence angle was estimated by the occultation of the mirror by the backplane's opposite rim, accounting for the known different level of the backplane surface with respect to the optical surface. The XSM was initially aligned at an incidence angle of 1.4 deg, and later increased to 2.7 deg to expand the trace in the MCP, increasing the image resolution.

Finally, for optics tests it is very important to keep the temperature stable within 1 °C and as close to the integration temperature (20 °C). The XACT facility was not designed, however, to be controlled in temperature. To maintain the temperature at the desired value, the entire experimental chamber was surrounded with metallic tubes in which water at 20 °C is circulated. All the chamber was finally wrapped into some layers of thermal insulator. In this way, the temperature of the modules under test (as measured by a sensor placed on the alignment stage) could always be maintained between 19.5 °C and 21 °C.

## 5. X-RAY TESTS AND SHAPE DRIVE

### 5.1. XMP

After alignment, the XMP was entirely recorded in all its length with all piezos at 0 V, always in X-ray illumination at 0.3 keV. Since the MCP has a diameter of 4 cm and the entire trace is approximately 20 cm long, the trace needed to be scanned with exposures separated by 2 cm to allow the image overlapping. The resulting mosaics for the parabola (Fig. 11) and the hyperbola (Fig. 12) are not perfect, but already show marked striations of the traces caused by profile errors. Scattering is negligible, but the surfaces appear deformed specially in their center, where the intensity dip denotes a large excess of convexity in the longitudinal direction. This location corresponds to the “M” piezo arrays on both surfaces, and the convexity was already observed in the LTP measurements. Another intensity minimum appears on the left side, induced by the “L” piezos. The region occupied by the “S” piezos appears much more uniform, as it was expected from the comparatively smaller deformation measured with the LTP (Sect. 2.2).

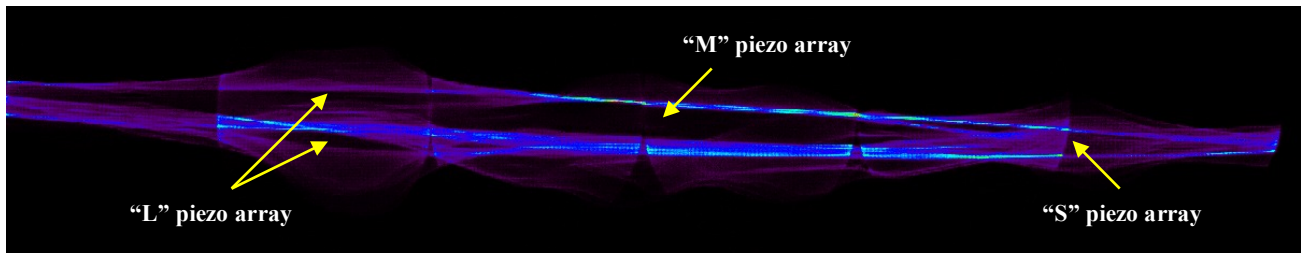


Fig. 11: a mosaic of single MCP exposures of the parabola in the XMP, returning the entire trace length at 0.3 keV. The bright and dark lines are a consequence of the mirror deformations in the longitudinal direction. We note the dark zones related to a large convexity excess induced by the glue shrinkage by the “M” and “L” piezos. The discontinuities in the striations are junctions between adjacent exposures.

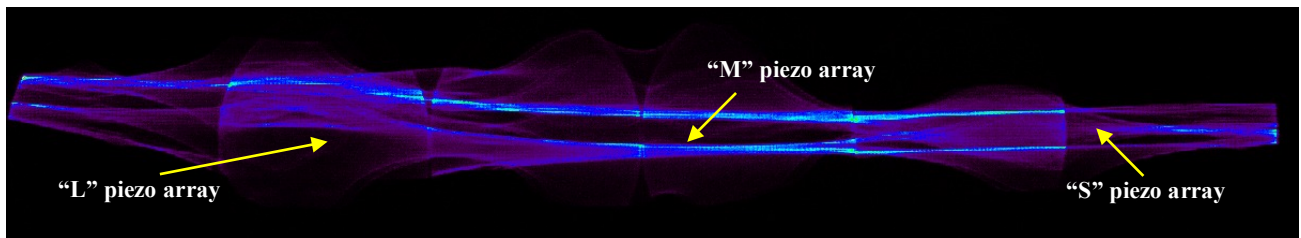


Fig. 12: a mosaic of single MCP exposures of the hyperbola in the XMP, returning the entire trace length at 0.3 keV. We note a similar behavior as in the parabola (Fig. 11).

Acting on the voltages does not change the intensity variation noticeably in the “L” and “M” regions. In contrast, the regions corresponding to the piezo array “S” change the striation pattern when the piezos are energized. For example, in the hyperbolic segment, we see (Fig. 13) the evolution of the intra-focal pattern as the feeding voltages shift toward negative values. At 0 V, the deformation caused by the glue is clearly seen, and the resulting trace broadening is difficult to interpret. The situation becomes worse when all the piezos are fed at positive voltages: this is visible from the further broadening of the intensity filaments. Turning all the piezo voltages at -90 V, the deformation is partly corrected as the

width becomes close to the nominal one and the intensity striations tend to become parallel to the azimuthal direction. A similar behavior is observed in the parabolic sector (Fig. 14). Also in this case, the correction is not complete, because the trace shrinks but still remain of non-uniform intensity. The final striations, moreover, still cross each other; hence, a quantitative analysis to derive the actual mirror profile is not possible.

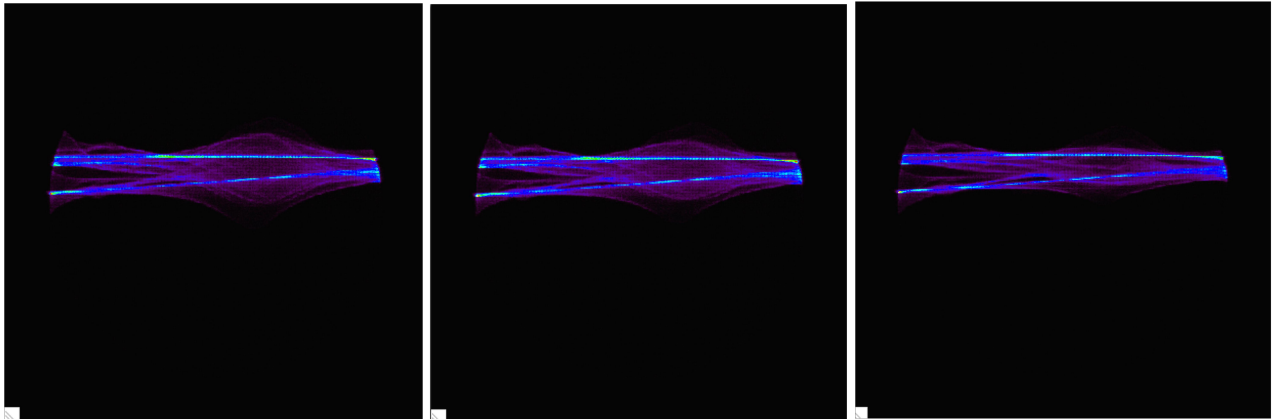


Fig. 13: exposure of the “S” mirror sector on the *hyperbolic* segment of the XMP: (left) all the S piezos at +60 V, (center) all the S piezos at 0 V, (right) all the piezos at -90 V. A partial correction of the trace broadening induced by the glue shrinkage is obtained by feeding the piezos at negative voltages.

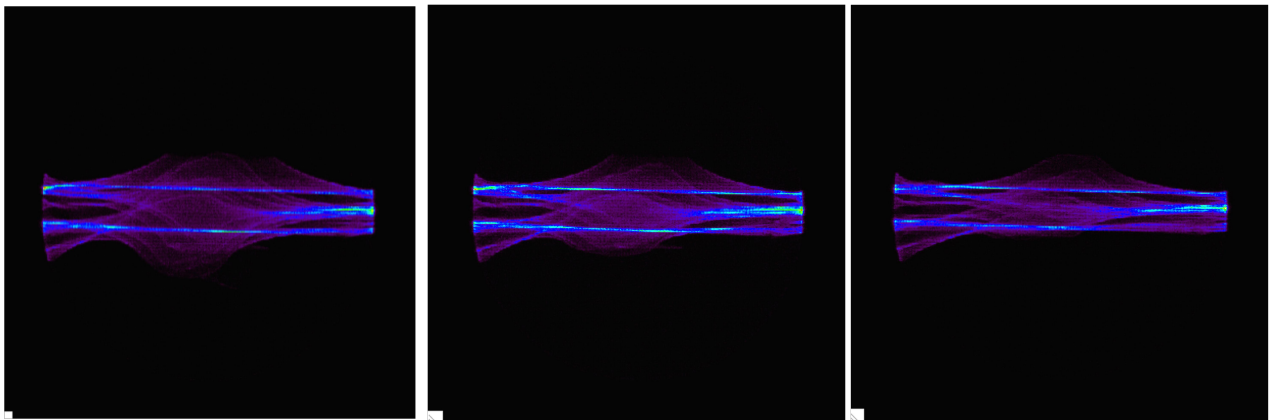


Fig. 14: exposure of the “S” mirror sector on the *parabolic* segment of the XMP: (left) all the S piezos at +60 V, (center) all the S piezos at 0 V, (right) all the piezos at -90 V. A partial correction of the trace broadening induced by the glue shrinkage is obtained by feeding the piezos at negative voltages, although less effective than in the hyperbola case (Fig. 13).

### 5.1. XSM

In the XSM tests, the two sectors have been illuminated at 0.3 keV separately. Measuring the first sector, the mirror was aligned at 1.4 deg with respect to the incident beam. The trace has a width already close to the nominal width, but the local deformations caused by the piezoelectric patches are visible as striation broadenings in the central regions. We have activated a piezo at a time at negative voltages, and observed the modification of the intensity distribution. Some pictures are shown in Fig. 15: the reduction of the trace broadening is visible at the location of the activated piezoelectric patch.

After re-aligning the XSM at 2.7 deg, the second sector was illuminated with X-rays. Also in this case, the deformations imparted by the glue are visible as “swollen” lines crossing each other. Having increased the incidence angle, the mirror section (Fig. 16) has become almost twice as large as the one shown in Fig. 15. The trace enlargement provides more detail on the profile deformations. Feeding all the piezo of the array at negative voltages, the profile defects are progressively corrected, although not completely. Also in this case, the intensity lines still cross each other, therefore the intensity profile cannot be used to affordably derive the mirror shape and so determine the detailed voltages to apply.

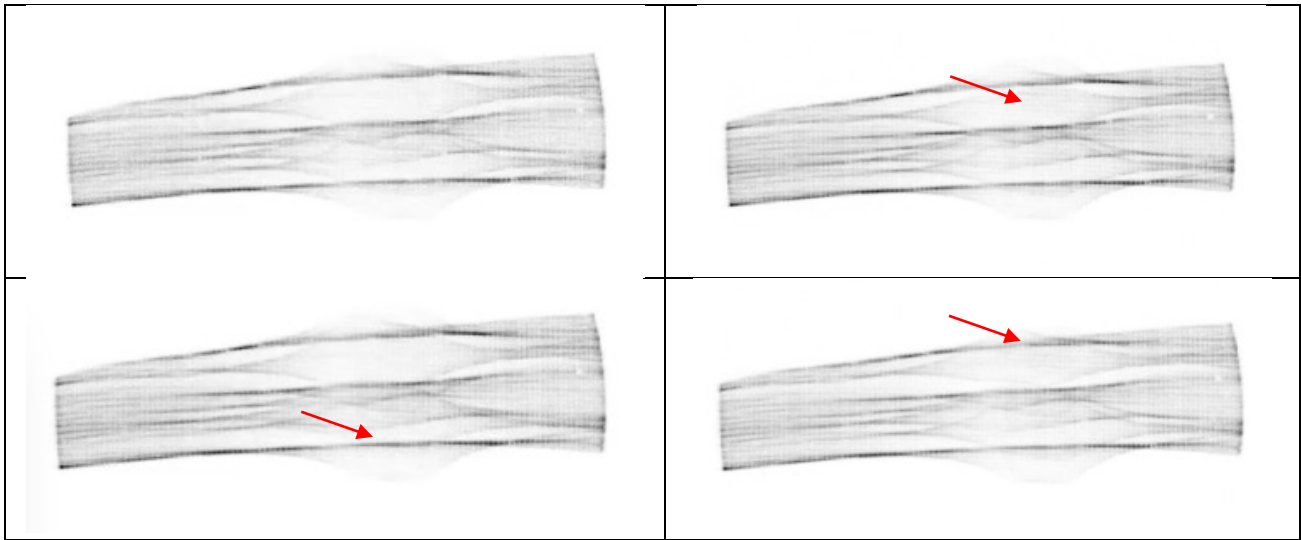


Fig. 15: first sector of the XSM: illuminated at 0.3 keV: activation in sequence of the 7 piezos at -60 V, at 1.4 deg incidence angle. We show (arrows) the activation of the 7<sup>th</sup> (top right), the 2<sup>nd</sup> (bottom left), and the 8<sup>th</sup> (bottom right). The local deformations introduced by the piezos is reduced as they are energized at negative voltages.

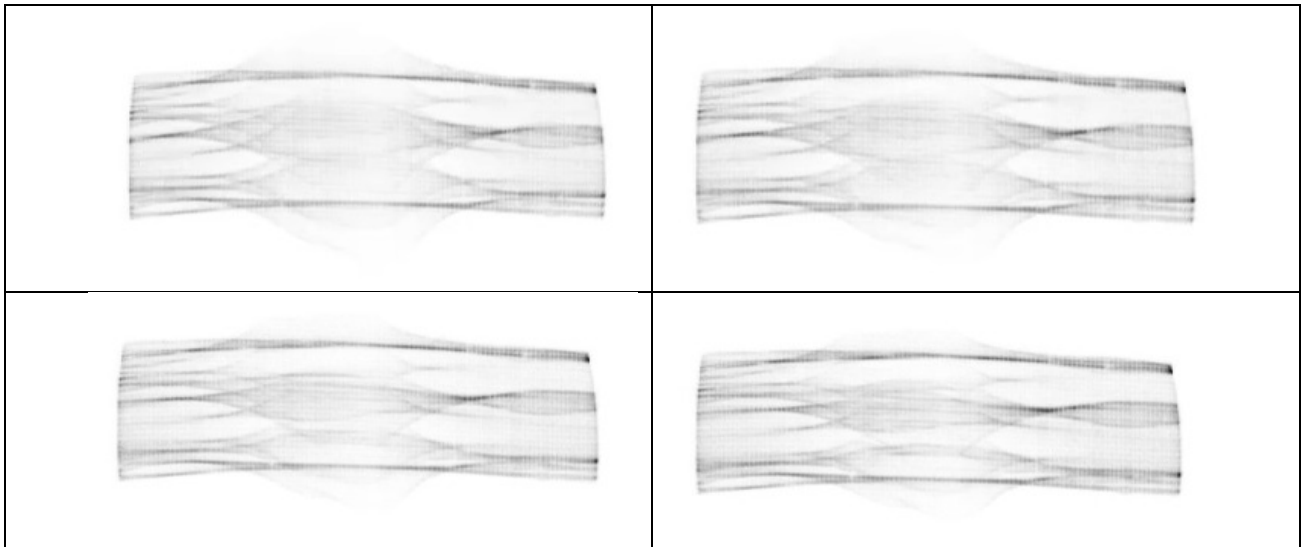


Fig. 16: second sector of the XSM, illuminated at 0.3 keV: voltage ramp of the 7 piezos together at 0 V (top left), -60 V (top right), -80 V (bottom left), -90 V (bottom right), at an incidence angle of 2.7 deg. We note the deformations induced by the glue on the glass foil, visible as broadening of the striations, progressively corrected for increasing negative voltages.

## 6. CONCLUSIONS

We have manufactured a few active X-ray mirror prototypes, using an approach based on the activation of lightweight X-ray optics made of slumped glasses, using tangential piezo components and the XACT test facility to perform intra-focal X-ray tests. We have developed a method to bring the voltages to the piezo elements via non-obstructing electrodes deposited by photolithography, modified the integration procedure of the slumped glasses to apply the piezoelectric patches to the non-reflective side of the mirror without interfering with the ribs, minimizing the glue thickness and preserving the electrical contact of the piezos with the electronic board used to provide the desired voltages. Among the ones used, the smallest piezos correctly react to the application of voltages in the range  $\pm 90$  V, deforming locally the mirror in both directions, and the change of shape is visible in X-ray illumination when the reflected beam is observed in intra-focal position. However, the glue shrinkage and nonuniformity still deform the mirror to an extent that can be corrected only

partially, and the intensity distribution in the X-ray image is still too complicated to extract a reliable mirror profile from the data. Work is currently on-going to deal with a quantitative analysis from the last dataset; also other manufacturing methods of active X-ray optics, currently being studied and less prone to introduce mirror deformations, might benefit of the experience gained in this project.

## ACKNOWLEDGMENTS

The AXIOM project, devoted to the study of the correction of thin glass/plastic foils for X-ray mirrors, was financed in 2013-2016 by a TECNO-INAF 2012 grant.

## REFERENCES

- [1] Bavdaz, M., Wille, E., Shortt, B., et al., "The ATHENA optics development," Proc. SPIE 9905, 990525 (2016)
- [2] Collon, M.J., Vacanti, G., Günther, R., et al., "Silicon pore optics for the ATHENA telescope," Proc. SPIE 9905, 990528 (2016)
- [3] Craig, W.W., An, H., Blaedel, K.L., et al., "Fabrication of the NuSTAR flight optics," Proc. SPIE 8147, 81470M (2011)
- [4] Civitani, M., Basso, S., Ghigo, M., Pareschi, G., Salmaso, B., Spiga, D., Vecchi, G., Banham, R., Breuning, E., Burwitz, V., Hartner, G., Menz, B., "Cold and Hot Slumped Glass Optics with interfacing ribs for high angular resolution x-ray telescopes," Proc. SPIE 9905, 99056U (2016)
- [5] Salmaso, B., Basso, S., Civitani, M., Ghigo, M., Holyszko, J., Spiga, D., Vecchi, G., Pareschi, G., "Slumped glass optics development with pressure assistance," Proc. SPIE 9905, 990523 (2016)
- [6] Proserpio, L., Wen, M., Breuning, E., Burwitz, V., Friedrich, P., Madarasz, E., "Indirect slumping of D263 glass on Fused Silica mould," Proc. SPIE 9905, 99056Y (2016)
- [7] Salmaso, B., Basso, S., Civitani, M., Ghigo, M., Holyszko, J., Spiga, D., Vecchi, G., Pareschi, G., "Slumped glass foils as substrate for adjustable x-ray optics," Proc. SPIE 9965, 99650B (2016)
- [8] Spiga, D., Basso, S., Bavdaz, M., Burwitz, V., Civitani, M., Citterio, O., Ghigo, M., Hartner, G., Menz, B., Pareschi, G., Proserpio, L., Salmaso, B., Tagliaferri, G., Wille, E., "Profile reconstruction of grazing-incidence X-ray mirrors from intra-focal X-ray full imaging," Proc. SPIE 8861, 88611F (2013)
- [9] O'Dell, S., Aldcroft, T., Allured, R., Atkins, C., Burrows, D., et al., "Toward large-area sub-arcsecond x-ray telescopes," Proc. SPIE 9208, 920805 (2014)
- [10] Allured, R., Hertz, E., Marquez, V., Cotroneo, V., Wallace, M., Salmaso, B., Civitani, M., Trolier-McKinstry, S., Vikhlinin, A., Pareschi, G., Reid, P., "Laboratory demonstration of the piezoelectric figure correction of a cylindrical slumped glass optic," Proc. SPIE 9905, 990554 (2016)
- [11] Spiga, D., Barbera, M., Basso, S., Civitani, M., Collura, A., Dell'Agostino, S., Lo Cicero, U., Lullo, G., Pellicciari, C., Riva, M., Salmaso, B., Sciortino, L., "Active shape correction of a thin glass/plastic x-ray mirror," Proc. SPIE 9208, 92080A (2014)
- [12] Dell'Agostino, S., Riva, M., Spiga, D., Basso, S., Civitani, M., "Integrated modeling for parametric evaluation of smart x-ray optics," Proc. SPIE 9150, 915021 (2014)
- [13] Spiga, D., Barbera, M., Collura, A., Basso, S., Candia, R., Civitani, M., Di Bella, M., Di Cicca, G., Lo Cicero, U., Lullo, G., Pellicciari, C., et al., "Manufacturing and testing a thin glass mirror shell with piezoelectric active control," Proc. SPIE 9603, 96031N (2015)
- [14] Spiga, D., Barbera, M., Collura, A., Basso, S., Candia, R., Civitani, M., Di Bella, M., Di Cicca, G., Lo Cicero, U., Lullo, G., Pellicciari, C., Riva, M., Salmaso, B., Sciortino, L., Varisco, S., "Manufacturing an active X-ray mirror prototype in thin glass," Journal of Synchrotron Radiation 23(1), 59 (2016)
- [15] Collura, A., Barbera, M., Inzerillo, G., Mirabello, F., Sciortino, S., Serio, S., "X-ray Astronomy Calibration and Testing Facility (XACT) at Osservatorio Astronomico di Palermo G.S. Vaiana," Proc. SPIE 2280, 206 (1994)
- [16] Barbera, M., Candia, R., Collura, A., Di Cicca, G., Pellicciari, C., Sciortino, S., Varisco, S., "The Palermo XACT facility: a new 35 m long soft x-ray beam-line for the development and calibration of next-generation x-ray observatories," Proc. SPIE 6266, 62663F (2006)
- [17] Lo Cicero, U., Sciortino, L., Lullo, G., Di Bella, M., Barbera, M., Collura, A., Candia, R., Spiga, D., Basso, S., Civitani, M., Pellicciari, C., et al., "Electrical connections and driving electronics for piezo-actuated x-ray thin glass optics," Proc. SPIE 9965, this conference